Cavity ring-down spectroscopy of ^{15}N enriched N_2O near 1.56 μm

A.-W. Liu [a,b,*], C.-L. Hu [a], J. Wang [a], V.I. Perevalov [c], S.-M. Hu [a,b]

[a] *Hefei National Laboratory for Physical Sciences at Microscale, iChem Center, University of Science and Technology of China, Hefei 230026,China*
[b] *CAS Center for Excellence in Quantum Information and Quantum Physics, University of Science and Technology of China, Hefei 230026, China*
[c] *Laboratory of Theoretical Spectroscopy, V. E. Zuev Institute of Atmospheric Optics, Siberian Branch, Russian Academy of Sciences, 1, Akademicien Zuev sq., 634055, Tomsk, Russia*

ARTICLE INFO

ABSTRACT

The absorption spectrum of nitrous oxide around 1.56 μm has been recorded with Doppler limited resolution by a continuous-wave cavity ring-down spectrometer at room temperature using ^{15}N-enriched samples. The typical sensitivity was at the level of 2×10^{-10} cm^{-1}. In total, 3389 transitions were observed and ro-vibrationally assigned on the basis of the global effective Hamiltonian model for six nitrous oxide isotopologues ($^{14}N^{15}N^{16}O$, $^{15}N^{14}N^{16}O$, $^{14}N^{15}N^{18}O$, $^{15}N^{14}N^{18}O$, $^{14}N^{15}N^{17}O$ and $^{15}N^{14}N^{17}O$). The band-by-band analysis led to the determination of ro-vibrational parameters of 47 bands, 36 of them were newly observed, and the rotational analysis of 11 others were significantly extended and improved. New sets of the effective Hamiltonian parameters were determined for the $^{14}N^{15}N^{16}O$ and $^{15}N^{14}N^{16}O$ isotopic species.

© 2019 Elsevier Ltd. All rights reserved.

1. Introduction

Nitrous oxide is a minor constituent of the Earth atmosphere. Being a greenhouse gas it plays an important role in the atmospheric radiation balance. This molecule also contributes to the ozone layer depletion. In addition, nitrous oxide is one of the products of the burning of the organic fuels in the air. The high resolution spectra of this molecule can be used for the monitoring of its concentration in the atmosphere and in the combustion exhaust. $^{14}N^{15}N^{16}O$ and $^{15}N^{14}N^{16}O$ are the most abundant minor isotopic species of the nitrous oxide molecule. High resolution spectra of these isotopologues were extensively studied by us using Fourier transform spectroscopy and ^{15}N-enriched samples of nitrous oxide [1–3]. Using these results and line positions from other publications [4–20] we have obtained parameters of different polyads from the global effective Hamiltonians (EH) models for these isotopologues [21]. The CW-CRDS spectrometer with very high sensitivity elaborated in USTC [22,23] for the 1.56 μm region together with highly enriched in ^{15}N samples of nitrous oxide allowed us to detect very weak bands of these isotopologues which are very important for the improvement of the effective Hamiltonian parameters, or by other words for the im-

provement of the global modelling of the high resolution spectra of $^{14}N^{15}N^{16}O$ and $^{15}N^{14}N^{16}O$. The assigned weakest line was estimated to be 5.0×10^{-28} cm^{-1}/(molecule · cm^{-2}), which allowed the detection of several bands of the double substituted isotopic species $^{14}N^{15}N^{18}O$, $^{15}N^{14}N^{18}O$, $^{14}N^{15}N^{17}O$ and $^{15}N^{14}N^{17}O$ in this region for the first time.

Note that throughout the paper we use the notation for the isotopologues according to HITRAN [8]: $^{14}N^{15}N^{16}O$: 456, $^{15}N^{14}O^{16}O$: 546, $^{14}N^{15}N^{18}O$: 458, $^{15}N^{14}N^{18}O$: 548, $^{14}N^{15}N^{17}O$: 457, $^{15}N^{14}N^{17}O$: 547.

2. Experimental details

The scheme of the continuous-wave cavity ring-down spectrometer based on a tunable diode laser is very similar to that described in Refs. [24,25]. Briefly, the structure of the setup is as follows: a beam from the external diode laser (ECDL, Toptica DL Pro-1550) is coupled into a 86-cm-long resonance cavity. The ring-down cavity is composed of two mirrors with a high reflectivity of 99.996% at 1.56 μm (Layertec GmbH). The ring-down signal is detected by a photodiode and recorded by an analogue-digital converter (ADLink PCI 9846) installed on a personal computer. The ring-down curve is fit by an exponential decay function to derive the decay time τ, and the sample absorption coefficient α is determined according to the equation $\alpha = (c\tau)^{-1} - (c\tau_0)^{-1}$, where c is the speed of light and τ_0 is the decay time of an empty cavity.

---

* Corresponding author.
E-mail addresses: awliu@ustc.edu.cn (A.-W. Liu), clhu@mail.ustc.edu.cn (C.-L. Hu), jinwang@ustc.edu.cn (J. Wang), vip@iao.ru (V.I. Perevalov), smhu@ustc.edu.cn (S.-M. Hu).
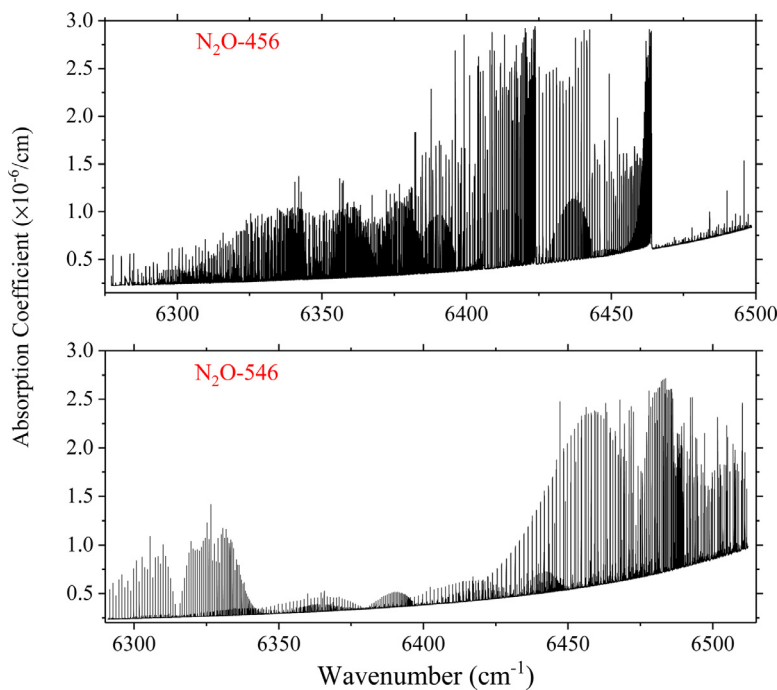
Fig. 1. Overview of the CW-CRDS spectrum of two ^{15}N substituted nitrous oxide samples between 1.54 and 1.59 μm. Upper panel: N₂O-456 enriched sample. Lower panel: N₂O-546 enriched sample, with the pressures in the range of 5.0 and 6.5 Torr.

The noise-equivalent absorption coefficient varies from 2×10^{-10} to 7×10^{-10} cm^{-1} depending on the reflectivity of the mirrors.

Two samples with 456 and 546 enriched nitrous oxide isotopes were purchased from Icon Services Inc., and further purified by a "freeze-pump-thaw" process before use. The stated isotopic concentrations of 456 and 546 are 99% in the respective samples. Sample pressures in the range of 5.0 and 6.5 Torr were adopted and the spectra were recorded at room temperature (295±1 K). The sample pressure was measured by a capacitance manometer (full range 10 kPa, 0.5% accuracy). The spectrum calibration was based on the readings given by a calibrated lambda-meter (Bristol 621A) with 60 MHz absolute accuracy.

An overview of the CW-CRDS spectra is presented in Fig. 1. A small part of the N₂O-456 spectrum in Fig. 2 illustrates the Q branch of the 4310 – 0110 band of N₂O-456 around 1.575 μm with a noise level of 2×10^{-10} cm^{-1}.

3. Rovibrational analysis

3.1. Vibrational assignment

The observed transitions were assigned on the basis of the predictions of the effective ro-vibrational Hamiltonian developed by Teffo et al. [26]. The sets of the effective Hamiltonian parameters for N₂O-456 and N₂O-546 were obtained by Tashkun et al. [21]. The adopted effective Hamiltonian is based on a polyad structure resulting from the approximate relations between the harmonic frequencies $\omega_3 \approx 2\omega_1 \approx 4\omega_2$. Due to the strong mixing between the normal mode $(V_1 V_2^{l_2} V_3)$ vibrational states, it is preferable to label the vibrational energy levels using the triplet $\{P = 2V_1 + V_2 + 4V_3, l_2, i\}$ where P is a polyad number and the index i increases with the energy at given P and l_2. Here l_2 is the vibrational angular momentum quantum number. We survey the vibrational assignments and the fraction relative to the $(V_1 V_2^{l_2} V_3)$ dominant basis states of the present studied upper vibrational levels in Table 1. A summary of the numbers of the transitions and

the bands of the different N₂O isotopologues obtained in this work in the 6277 - 6512 cm^{-1} region is given in Table 2.

3.2. Band by band rotational analysis

The standard expression of the vibration-rotation energy levels was applied for the fit of the spectroscopic parameters to the unperturbed bands:

$$E_v(J) = G_v + B_v J(J+1) - D_v J^2(J+1)^2 + H_v J^3(J+1)^3; \qquad (1)$$

where G_v is the vibrational term value, B_v is the rotational constant, Dv and Hv are centrifugal distortion constants. The spectroscopic parameters for an upper state were fitted directly to the observed line positions of the respective band, and in the case of hot band involving e and f rotational levels, the ee, ef, fe, and ff sub-bands were considered, independently. The lower state rotational constants were constrained to their literature values [13,14,19,20]. The observed and calculated line positions are included in the Supplementary Material (I) attached to this paper.

3.2.1. The 456 and 546 isotopologues

Twenty-four and seventeen bands were assigned for the 456 and 546 species, respectively. Some bands were previously observed by FTS with natural [9] and highly enriched in 456 [1] and 546 [2] nitrous oxide samples and by the CRDS [10,11] with natural nitrous oxide sample: four bands of 0003-0000 [1,9,10], 0113-0110 [1,10], 0223-0220 [1,11] and 4310-0110 [1] for 456 isotopologue; seven bands of 0003-0000 [2,10], 0113-0110 [2,10], 3400-0000 [2,10], 0203-0200 [2,11], 0223-0220 [2,11], 1003-1000 [2] and 3510-0110 [2] for 546 isotopologue. The upper vibrational states of some newly observed bands were studied previously [1,2] through other observed bands. These states are 0004, 5200, 6000, 2003, 3111, 1113 and 1511 belonging to 456 isotopologue. Three states of 2620, 3111 and 1113 are from the hot bands observation of 546 isotopologue. Therefore, the spectroscopic information of eight and ten vibrational states for 456 and 546 species, respectively, is determined for the first time. The spectroscopic parameters of 41 ob-

Table 1

Vibrational assignment and fractions respective to the basis states for the observed bands of N_2O-456 and N_2O-546 in the 6277–6512 cm^{-1} CRDS spectra.

ΔP[a]	Band[b]	(P, l_2, i)[c]	$E(P, l_2, i)$ (cm^{-1})[d]	Basis states[e]	%Fraction[f]
$^{14}N^{15}N^{16}O$					
10	3420–0000	(10 2 20)	6259.2389	$34^20/42^20/26^20$	38/31/23
11	1511 – 0000	(11 1 6)	6370.9508	$15^11/31^11$	35/29
12	0003 –0000	(12 0 1)	6446.8927	$00^\circ3$	99
11	3111 – 0000	(11 1 8)	6491.8306	$31^11/23^11$	55/33
12	0402 –0000	(12 0 2)	6500.5780	$04^\circ2/12^\circ2$	75/22
10	4310 – 0110	(11 1 12)	6924.1660	$43^10/51^10/35^10$	34/27/24
12	0113 – 0110	(13 1 1)	6981.8566	01^13	99
12	0512– 0110	(13 1 2)	7040.6189	$05^12/13^12$	67/28
10	5200 – 1000	(12 0 16)	7249.2424	$52^\circ0/60^\circ0/44^\circ0$	29/28/23
10	5200 – 0200	(12 0 16)	7249.2424	$52^\circ0/60^\circ0/44^\circ0$	29/28/23
10	6000 – 0200	(12 0 15)	7492.1209	$60^\circ0/36^\circ0$	47/20
12	0203 – 0200	(14 0 1)	7511.6364	$02^\circ3$	91
12	0223 – 0220	(14 2 2)	7519.7398	02^23	99
10	4420 – 0220	(12 2 27)	7520.4994	$44^20/36^20/52^20$	32/28/19
12	1003 – 1000	(14 0 3)	7650.7537	$10^\circ3$	90
12	0313 – 0310	(15 1 1)	8043.1930	03^13	86
12	0333 – 0330	(15 3 2)	8058.0751	03^33	98
10	5310 – 1110	(13 1 16)	8173.2580	$53^10/45^10/37^10/61^10$	28/27/18/16
12	1113 – 1110	(15 1 3)	8191.2479	11^13	85
12	0004– 0001	(16 0 1)	8538.5130	$00^\circ4$	98
12	0403 – 0400	(16 0 2)	8568.7473	$04^\circ3/12^\circ3$	75/20
12	1203 –1200	(16 0 4)	8722.9223	$12^\circ3/04^\circ3$	71/21
12	1223 – 1220	(16 2 7)	8732.5360	$12^23/04^23$	80/17
12	2003 – 2000	(16 0 7)	8844.7195	$20^\circ3$	79
$^{15}N^{14}N^{16}O$					
10	2620 – 0000	(10 2 20)	6283.3134	$34^20/26^20$	33/32
10	3400– 0000	(10 0 12)	6315.0108	$34^\circ0/42^\circ0/26^\circ0$	30/24/22
11	3111 – 0000	(11 1 6)	6401.6514	$31^11/15^11/07^11$	41/31/18
10	3510– 0110	(11 1 12)	6937.6721	$35^10/43^10/27^10$	31/23/23
12	0113 – 0110	(13 1 1)	7059.5383	01^13	96
12	0512– 0110	(13 1 2)	7114.6610	$05^12/13^12$	54/37
10	3620 – 0220	(12 2 27)	7552.8468	$36^20/28^20/44^20$	31/25/22
10	3600–1000	(12 0 16)	7576.1471	$36^\circ0/44^\circ0/28^\circ0$	28/25/19
10	3600 – 0200	(12 0 16)	7576.1471	$36^\circ0/44^\circ0/28^\circ0$	28/25/19
12	0203– 1000	(14 0 1)	7592.4865	$02^\circ3$	84
12	0203 – 0200	(14 0 1)	7592.4865	$02^\circ3$	84
12	0223 – 0220	(14 2 2)	7604.4192	02^23	96
12	1003 – 1000	(14 0 3)	7702.5014	$10^\circ3$	78
12	0313 – 0310	(15 1 1)	8129.1124	$03^13/11^13$	76/19
12	0333 – 0330	(15 3 2)	8150.6173	03^33	96
12	1113 – 1110	(15 1 3)	8253.9048	$11^13/03^13$	70/21
12	0004– 0001	(16 0 1)	8628.6834	$00^\circ4$	93

[a] Band series.

[b] According to the maximum value of the modulo of the expansion coefficients of the eigenfunction.

[c] Cluster labelling notation $(P = 2V_1 + V_2 + 4V_3, l_2, i)$ for the upper state of the band.

[d] H^{eff} calculated energy of the vibration-rotation state (P, l_2, i).

[e] Only basis states with modulo of expansion coefficients larger than 0.4 are presented.

[f] Squares of the expansion coefficients of the upper vibrational state for the dominant basis states appearing in the preceding column.

Table 2

Summary of the number of the transitions and bands of the different N_2O isotopologues obtained in this work by CRDS in the 6277 - 6512 cm^{-1} region.

Isotopologue	HITRAN notation	Number of bands		Number of transitions
		This work	Literature	
$^{14}N^{15}N^{16}O$	456	24	4 [1,9–11]	1529
$^{15}N^{14}N^{16}O$	546	17	7 [2,10,11]	1389
$^{14}N^{15}N^{18}O$	458	2	0	241
$^{15}N^{14}N^{18}O$	548	1	0	73
$^{14}N^{15}N^{17}O$	457	2	0	112
$^{15}N^{14}N^{17}O$	547	1	0	45
		47	11	3389

served bands for 456 and 546 isotopologues, respectively, are presented in Tables 3 and 4. It is worth noting that three of the bands of the 456 and 546 isotopologues were found rising from (0310), (0330) lower states. Though these two lower states were not reported previously, the observed transitions allowed us to obtain

the spectroscopic constants of these lower states. The differences between the upper and lower vibrational term values were determined, which are listed together with B_v and D_v in Tables 3 and 4. Notice that the vibrational term values for the (0310) state of the 456 isotopologue, the (0330) state of the 546 isotopologue could
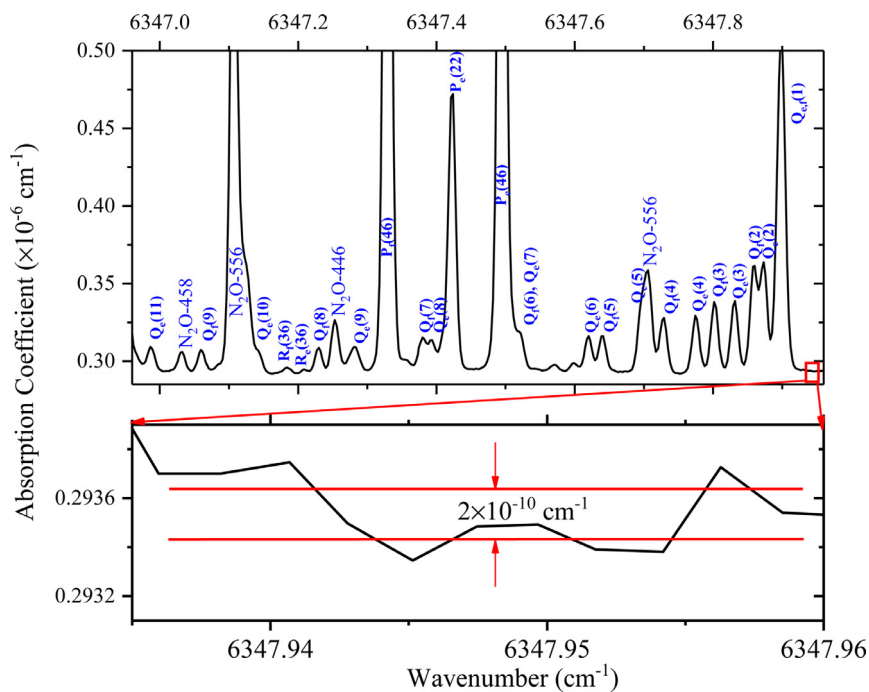
Fig. 2. A small part of N_2O-456 spectra around 6347.0 cm^{-1} was mainly assigned to the Q branch of the 4310 – 0110 band. We use the simplified notations for Q-lines: $Q_e \equiv Q_{f \leftarrow e}$ and $Q_f \equiv Q_{e \leftarrow f}$. Five transitions of $P_{e,f}(46)$, $P_e(22)$ and $R_{e,f}(36)$ belong to 0113 – 0110, 1003 – 1000, and 1113 – 1110 hot bands, respectively. The enlargement illustrates the noise level of 2.0×10^{-10}/cm.

be indirectly derived from Amiot's work [13] to be 1714.0238 and 1756.5762 cm^{-1}, respectively.

In this work, four states were found to be affected by some perturbations, while two of them have already been observed in our previous FTS studies [1,2]. For example, the 1511 state of N_2O-456 isotopologue was perturbed by the 0(11)10 state due to the intrapolyad resonance anharmonic interaction. The energy levels difference between the 1511 ((11 1 6)) and 0(11)10 ((11 1 7)) states at $J = 1$ is only 0.858 cm^{-1}, but grows with the increasing of J values being 12.837 cm^{-1} at $J = 50$. The effective Hamiltonian model including this intrapolyad interaction helped us identify some weak transitions of the 1511 – 0000 band in the $\Delta P = 12$ strong absorption region. The spectroscopic constants of the 1511 state in Table 3 should be used with caution because of an anomalous large value of the centrifugal distortion constant H_v. The 0003, 3600, 3620 vibrational states of N_2O-546 species are affected by the interpolyad resonance interactions. Table 5 summarizes these bands together with the perturbation mechanisms and J values at which the energy level crossings take place.

3.2.2. The 458, 457, 548 and 547 minor isotopologues

The spectroscopic knowledge of these four minor isotopologues was limited in the mid-infrared region. More than 40 years ago, Amiot [13,14] performed the analysis of the FTS spectra recorded with the ^{15}N enriched nitrous oxide samples, which provided the spectroscopic constants of 10, 9, 3, and 3 vibrational states for N_2O-458, 548, 457 and 547 species, respectively. Two more vibrational states of N_2O-458 and 548 were reported in our FTS measurements with ^{15}N enriched nitrous oxide samples [3]. A total of six unperturbed bands of these four minor isotopologues are newly observed here by CRDS. The spectroscopic parameters related to the 458, 548, 457 and 547 species are presented in Table 6. Note that it is the first observation of the hot band for the 457 species. And the absolute values of the residuals between the experimental and calculated line positions in more than 90% cases are located between 0.006 and 0.014 cm^{-1}, more than three

times of our experimental uncertainty, if the ground state spectroscopic constants of 547 isotopologue [13] was used in the analysis of 0003 – 0000 band. Therefore, the spectroscopic constants of the lower 0110 and 0000 vibrational states for 457 and 547, respectively are re-determined by fitting the data with the relation: $\Delta_2 F'' = (4B'' - 6D'')(J + \frac{1}{2}) - 8D''(J + \frac{1}{2})^3$, where J is the rotational quantum number of the upper energy level. The retrieved lower state parameters are also given in Table 6.

4. Effective Hamiltonian parameters

The new observed bands for the $^{14}N^{15}N^{16}O$ and $^{15}N^{14}N^{16}O$ isotopologues allow refining the parameters of the global polyad models of the effective Hamiltonian for these isotopologues. The latest sets of the EH parameters for them [4] were found by the fittings to the line positions determined by us from FTS spectra [1–3] and to those collected from the literature [4–20]. Since that time four additional papers were published [25,27–29] in which the line positions of several bands of these isotopologues were determined using the CRDS technique. It is necessary to emphasize that Song et al. [25] have studied the fifth overtone bands ($6\nu_3$) of these isotopologues with the band centers at 12,636.206 cm^{-1} and at 12,766.196 cm^{-1}, respectively. The 0006 vibrational state is the highest vibrational state ever observed. All these new data were involved in the new fittings. We used the polyad model of effective Hamiltonian [21,26] and GIP computer code [30] for the least-squares fitting its parameters.

The aim of the fitting procedure was to minimize the weighted standard deviation χ defined according to the usual formula

$$\chi = \sqrt{\frac{\sum_{i \leftarrow j=1}^{N} \left[\left(\nu_{i \leftarrow j}^{obs} - \nu_{i \leftarrow j}^{calc} \right) / \delta_{i \leftarrow j} \right]^2}{N - n}}, \tag{2}$$

where $\nu_{i \leftarrow j}^{obs}$, $\nu_{i \leftarrow j}^{calc}$ are the observed and calculated line positions, respectively, and $E_v(J) = G_v + B_v J(J+1) - D_v J^2(J+1)^2 + H_v J^3(J+1)^3$; is the uncertainty of the observed line position. N is the numbea of

Table 3
Spectroscopic parameters (in cm^{-1}) of the rovibrational bands of N$_2$O-456 recorded by CRDS between 6277 and 6499 cm^{-1}.

	Lower states constants [17,20]				
	State		G_v	B_v	$D_v \times 10^7$	$H_v \times 10^{12}$
	$V_1V_2\ l_2V_3$	(P, l_2, i)				
	0000e	(0 0 1)	0.0	0.418 981 810	1.763264	
	0110e	(1 1 1)	575.43365	0.419 089 600	1.785826	
	0110f	(1 1 1)	575.43365	0.419 918 641	1.794459	
	0200e	(2 0 1)	1144.33338	0.419 921 722	2.845420	6.6796
	0220e	(2 2 2)	1151.03090	0.420 032 300	0.954000	
	0220f	(2 2 2)	1151.03090	0.420 034 800	1.813000	
	1000e	(2 0 2)	1280.35412	0.417 127 307	1.754555	4.7195
	1110e	(3 1 2)	1860.19121	0.417 273 136	1.773906	
	1110f	(3 1 2)	1860.19121	0.418 165 235	1.760323	
	0001e	(4 0 1)	2177.65681	0.415 654 098	1.756773	1.2541
	0400e	(4 0 2)	2278.19266	0.420 684 310	5.029130	3.0009
	1200e	(4 0 3)	2431.32249	0.418 090 902	2.744112	4.2985
	1220e	(4 2 5)	2439.59880	0.418 286 100	1.874700	3.1770
	2000e	(4 0 4)	2552.40820	0.415 298 300	1.73057	0.2578

ΔG_v [a]	Type	$V_1V_2\ l_2V_3$ [b]	(P, l_2, i)	G_v	B_v	$D_v \times 10^7$	$H_v \times 10^{12}$	Observed lines	n/N [c]	Rms $\times 10^3$
Cold bands										
6259.2389(78)	Δ-Σ	3420e – 0000e	(10 2 20)	6259.2389(78)	0.413369(13)	0.926(67)	−4.9(10)	R58	16/16	0.8
6370.1287(12)	Π–Σ	1511e – 0000e	(11 1 6)	6370.1287(12)	0.413063(15)	9.71(42)	419(33)	P63/R43	17/37	1.6
6446.89416(32)	Σ–Σ	0003e –0000e	(12 0 1)	6446.89416(32)	0.40897232(30)	1.74237(50)		P81/R84	139/143	0.8
6491.01046(58)	Π–Σ	3111e – 0000e	(11 1 8)	6491.01046(58)	0.4104353(25)	1.672(11)		P40/R9	24/34	1.2
6500.57789(71)	Σ–Σ	0402e–0000e	(12 0 2)	6500.57789(71)	0.4143335(31)	5.120(33)	35.37(89)	P52	39/44	1.0
Hot bands										
6287.07521(61)	Σ–Σ	5200e – 1000e	(12 0 13)	7567.42933(61)	0.4092293(26)	0.819(25)	10.77(65)	P6/R52	45/45	0.7
6290.50041(92)	Δ–Δ	1223e – 1220e	(16 2 7)	8730.09921(92)	0.4085164(49)	1.849(40)	*3.1770*	P11/R34	17/17	2.7
6291.5919(11)	Σ–Σ	1203e –1200e	(16 0 4)	8722.9144(11)	0.408288(82)	2.00(13)	29.4(54)	P7/R40	15/25	2.9
6292.30529(98)	Σ–Σ	2003e – 2000e	(16 0 7)	8844.71349(98)	0.4052475(64)	1.623(59)	*0.2578*	P8/R32	12/21	2.0
6312.24719(68)	Π–Π	5310e – 1110e	(13 1 16)	8172.43840(68)	0.4090266(34)	1.504(21)		P24/R39	28/37	1.4
6312.24920(66)		5310f – 1110f		8172.44041(66)[e]	0.4109746(29)	0.729(24)		P28/R36	34/39	1.3
6326.37086(60)	Φ–Φ	0333e – 0330e	(15 3 2)		0.4108934(22)	1.525(14)		P35/R40	42/44	0.8
6328.35211(49)	Π–Π	0313e – 0310e	(15 1 1)	8042.37591(49)[d]	0.4099488(13)	2.2504(71)	*2.16*	P38/R44	53/58	1.5
6328.35425(65)		0313f – 0310f		8042.37805(65)[d]	0.4114105(44)	2.055(66)	13.2(24)	P34/R43	48/61	1.4
6330.24298(74)	Π–Π	1113e – 1110e	(15 1 3)	8190.43419(74)	0.4073970(28)	1.734(20)		P39/R36	33/43	1.2
6330.24168(78)		1113f – 1110f		8190.43289(78)	0.4082263(29)	1.712(22)		P37/R36	35/43	1.2
6347.78890(67)	Σ–Σ	6000e – 0200e	(12 0 15)	7492.12228(67)	0.4104462(22)	2.525(14)	*6.6796*	P43/R38	39/39	1.1
6347.91229(57)	Π–Π	4310e – 0110e	(11 1 12)	6923.34594(57)	0.4104504(12)	1.4227(520)		P51/R46	70/79	1.3
6347.91442(51)		4310f – 0110f		6923.34807(51)	0.4120769(19)	1.141(17)	2.23(40)	P56/R53	81/86	1.3
6360.85533(64)	Σ–Σ	0004e – 0001e	(16 0 1)	8538.51214(64)	0.40562286(26)	1.743(19)	*1.2541*	P38/R36	40/43	0.8
6366.24588(53)	Δ–Δ	0223e – 0220e	(14 2 2)	7517.27678(53)	0.4102494(17)	0.898(13)	−0.32(25)	P62/R52	73/86	1.5
6366.99782(49)	Δ–Δ	4420e – 0220e	(12 2 27)	7518.02872(49)	0.4119125(11)	1.1485(50)		P53/R50	56/70	1.4
6366.99655(46)		4420f – 0220f		7518.02745(46)	0.41191632(85)	1.3267(27)		P61/R49	56/64	1.3
6367.30521(45)	Σ–Σ	0203e – 0200e	(14 0 1)	7511.63859(45)	0.41013484(75)	2.8254(23)	*6.6796*	P56/R60	74/84	1.5
6370.40091(49)	Σ–Σ	1003e – 1000e	(14 0 3)	7650.75503(49)	0.4070970(17)	1.686(14)	4.20(30)	P60/R43	68/81	1.6
6406.42292(43)	Π–Π	0113e – 0110e	(13 1 1)	6981.85657(43)	0.40922999(46)	1.76075(95)		P72/R73	96/108	1.1
6406.42133(38)		0113f–0110f		6981.85498(38)	0.40999766(45)	1.77684(97)		P72/R70	102/112	1.1
6423.09573(56)	Σ–Σ	5200e – 0200e	(12 0 13)	7567.42911(56)	0.4092280(22)	0.810(15)	*6.6796*	P41/R34	45/45	1.2
6464.3830(13)	Σ–Σ	0403e – 0400e	(16 0 2)	8742.5757(13)[f]	0.4156435(90)	8.52(16)	100.5(82)	R35	30/34	1.7
6465.18523(63)	Π–Π	0512e – 0110e	(13 1 2)	7040.61888(63)	0.4136616(25)	2.795(19)		P34/R37	49/52	1.3
6465.18463(69)		0512f – 0110f		7040.61828(69)	0.4158673(39)	3.043(53)	6.2(19)	P35/R43	50/56	1.3

The uncertainties are given in parenthesis in the unit of the last quoted digit.

[a] Difference between the upper and lower vibrational term values.

[b] Normal mode labeling according to the maximum value of the modulo of the expansion coefficients of an eigenfunction.

[c] n: number of transitions included in the fit; N: number of assigned rotational transitions.

[d] The vibrational term values should be used with caution because of the indirect rotational constants of the lower vibrational state.

[e] The vibrational term value is not given due to the absence of the respective value for the lower vibrational state.

[f] The vibrational term value should be used with caution since only the line positions of R branch were used for the spectroscopic constant determination.

the line positions in the datafile, and n is the number of the adjusted Hamiltonian parameters.

To describe the quality of a fit we use two additional values: root mean square (RMS) of the residuals of the fit and RMS of the residuals for a given source. These characteristics are defined according to the equation

$$RMS = \sqrt{\frac{\sum_{i \leftarrow j=1}^{N} \left(\nu_{i \leftarrow j}^{obs} - \nu_{i \leftarrow j}^{calc}\right)^2}{N}}, \qquad (3)$$

where N is the number of the fitted line positions in the first case and the number of the line positions of a source in the second case. The results of the line position fits for both isotopologues are given in Table 7.

4.1. The 456 isotopologue

The input datafile includes observed line positions collected from the literature [1,3,6–12,16–20,25,27–29] and those obtained in this work. The file contains near 30,300 lines and covers 12.6 – 12,640 cm^{-1} spectral range. A summary of the datafile is given in

Table 4

Spectroscopic parameters (in cm^{-1}) of the rovibrational bands of N_2O-546 recorded by *CW*-CRDS between 6291 and 6512 cm^{-1}.

		Lower states constants [17,20]							
		State		G_v	B_v	$D_v \times 10^7$	$H_v \times 10^{12}$		
		$V_1V_2\ l_2V_3$ [b]	(P, l_2, i)						
		0000e	(0 0 1)	0.0	0.408 857,965	1.642938			
		0110e	(1 1 1)	585.31212	0.405 037 265	1.656798			
		0110f		585.31212	0.405 781 109	1.667421			
		0200e	(2 0 1)	1159.97171	0.405 712 750	2.227530	2.2070		
		0220e	(2 2 2)	1170.84300	0.405 955(14)	1.55(10)	6.5(20)		
		0220f		1170.84300	0.405 950 4	1.691			
		1000e	(2 0 2)	1269.89198	0.403 263 601	1.597707	3.6343		
		0310e	(3 1 1)	1736.64780	0.405410775	1.914464			
		0310f		1736.64792	0.406 798 997	1.995707			
		1110e	(3 1 2)	1862.76703	0.403 489 984	1.61574			
		1110f		1862.76708	0.404 358 898	1.577311			
		0001e	(4 0 1)	2201.60529	0.401 497 172	1.640337	2.3380		
ΔG_v [a]	Type		(P, l_2, i)	G_v	B_v	$D_v \times 10^7$	$H_v \times 10^{12}$	*Observed lines*	n/N [c]	Rms $\times 10^3$
Cold bands										
6281.2864(28)	Δ-Σ	2620e – 0000e	(10 2 20)	6281.2864(28)	0.4010598(84)	1.204(71)	−13.2(18)	R48	28/30	0.9
6315.01566(58)	Σ–Σ	3400e – 0000e	(10 0 12)	6315.01566(58)	0.3994225(14)	0.3513(84)	5.19(13)	P6/R67	49/52	0.6
6400.0852(17)	Π–Σ	3111e – 0000e	(11 1 6)	6400.0852(17)	0.398808(13)	2.11(24)		P21/R26	11/17	1.4
Hot bands										
6306.24001(60)	Σ–Σ	3600e –1000e	(12 0 16)	7576.13199(60)	0.3990360(38)	0.253(51)	12.0(18)	P17/R44	52/55	0.8
6379.59829(75)	Δ–Δ	3620e – 0220e	(12 2 27)	7550.44129(75)	0.4002076(40)	1.863(39)		P32/R31	36/43	1.2
		3620f – 0220f		7550.43978(91)	0.4001972(77)	0.53(16)	−24.7(86)	P32/R34	37/45	1.4
6389.28222(45)	Φ–Φ	0333e – 0330e	(15 3 2)	8145.85842(45) [d]	0.39672011(96)	1.4606(36)		P47/R55	70/73	1.3
6391.67144(53)	Π–Π	0313e – 0310e	(15 1 1)	8128.31924(53)	0.3956858(12)	1.9124(52)		P51/R49	66/78	1.0
6391.67031(53)		0313f – 0310f		8128.31823(53)	0.3970111(17)	2.106(10)		P49/R44	47/58	1.3
6390.35681(76)	Π–Π	1113e – 1110e	(15 1 3)	8253.12384(76)	0.3934867(18)	1.5501(80)		P44/R48	36/51	1.8
6390.35363(70)		1113f – 1110f		8253.12071(70)	0.3942946(18)	1.5240(86)		P50/R41	33/48	1.4
6322.59742(93)	Σ–Σ	0203e – 1000e	(14 0 1)	7592.48940(93)	0.3958222(67)	1.87(11)	−12.5(46)	P29/R40	16/24	1.5
6351.56449(46)	Π–Π	3510e – 0110e	(11 1 12)	6936.87661(46)	0.3987288(20)	1.037(19)	2.16(50)	P53/R52	95/100	1.2
6351.56366(46)		3510f – 0110f		6936.87578(46)	0.4008559(19)	0.621(17)	1.97(42)	P55/R51	95/97	0.9
6416.15944(69)	Σ–Σ	3600e – 0200e	(12 0 16)	7576.13115(69)	0.3990374(48)	0.329(52)	2.207	P32/R24	27/30	1.0
6427.07976(68)	Σ–Σ	0004e – 0001e	(16 0 1)	8628.68505(68)	0.3914114(32)	1.675(28)	2.338	P36/R32	36/40	1.3
6431.20148(47)	Δ–Δ	0223e – 0220e	(14 2 2)	7602.04448(47)	0.3960781(17)	1.522(15)	6.16(35)	P56/R55	96/102	0.9
6432.51062(41)	Σ–Σ	0203e – 0200e	(14 0 1)	7592.48773(41)	0.3958403(13)	2.2221(88)	2.11(16)	P65/R56	97/105	1.1
6432.60962(42)	Σ–Σ	1003e – 1000e	(14 0 3)	7702.50160(42)	0.3931070(10)	1.5668(45)	3.6343	P53/R42	75/86	1.0
6473.43584(41)	Π–Π	0113e – 0110e	(13 1 1)	7058.74796(41)	0.39506867(58)	1.6442(14)		P69/R46	80/95	1.4
6473.43543(40)		0113f–0110f		7058.74755(40)	0.39577459(49)	1.6607(11)		P70/R69	96/106	1.1
6528.5678(47)	Π–Π	0512e – 0110e	(13 1 2)	7113.8799(47)	0.399323(13)	2.094(83)		P36	9/12	1.5
6528.5603(73)		0512f – 0110f		7113.8724(73)	0.401281(22)	2.53(16)		P33	10/12	1.6

The uncertainties are given in parenthesis in the unit of the last quoted digit.

[a] Difference between the upper and lower vibrational term values.

[b] Normal mode labeling according to the maximum value of the modulo of the expansion coefficients of an eigenfunction.

[c] *n*: number of transitions included in the fit; *N*: number of assigned rotational transitions.

[d] The vibrational term values should be used with caution because of the indirect rotational constants of the lower vibrational state.

Table 5

Observed interpolyad perturbations of the N_2O-546 bands between 6291 – 6512 cm^{-1}.

Band affected	Center (cm^{-1})	Resonance interaction mechanism	J_{cross} [a]	Ref. [b]
0003e-0000e	6515.9876	Interpolyad Coriolis (12 0 1)↔ (11 1 8)	56	[21]
3600e-1000e	6306.2400	Interpolyad anharmonic	62	
3600e-0200e	6416.1594	(12 0 16)↔ (14 0 1)		
3620e-0220e	6379.5983	Interpolyad Coriolis	88	
3620f-0220f	6379.5983	(12 2 27)↔ (13 19)	61	

[a] Value of the angular momentum quantum number at which the energy level crossing takes place.

[b] Previous reference in which the perturbation of the upper state was observed.

Table 8. The data file was augmented with a number of calculated line positions taken from Toth's calculated datafile SISAM.N2O [4] and marked as CALC in the second column of Table 8. These positions were calculated from spectroscopic constants. For the sake of weighting we assumed an uncertainty of 0.001 cm^{-1} for these data. The measurement uncertainties are listed in column 3 of the table. As the initial set of the effective Hamiltonian parameters, we used the set published in our previous paper [21]. With 133 parameters we have reached a global RMS=0.0013 cm^{-1}. The weighted standard deviation of the fit is χ =1.18. It does mean that the fit practically reaches the experimental accuracy. Note that 2192 badly measured or strongly perturbed lines were excluded from the fit. The root mean square of the residuals for each source is given in the last column of Table 8. The residuals are plotted versus wavenumber in the upper panel of Fig. 3.The fitted set of the effective Hamiltonian parameters is presented as Supplementary Material.

Table 6

Spectroscopic parameters (in cm^{-1}) of the rovibrational bands of N_2O −458, 457, 548, and 547 species recorded by CRDS between 6277 and 6512 cm^{-1}.

Lower states constants [13,14]

	Isotopologues	State		G_v	B_v	$D_v \times 10^7$	$H_v \times 10^{12}$
		$V_1V_2\ l_2V_3$	$(P,\ l_2,\ i)$				
		0000e	(0 0 1)	0.0	0.3954676	1.584	
	458	0110e	(1 1 1)	570.7780	0.395611	1.606	
		0110f		570.7780	0.396337	1.599	
		0000e	(0 0 1)	0.0	0.40660800	1.682	
	457	0110e*	(1 1 1)		0.406724(62)	1.68(65)	
		0110f*			0.408362(88)	3.2(12)	
	548	0000e	(0 0 1)	0.0	0.3819194	1.467	
	547	0000e*	(0 0 1)	0.0	0.393210(22)	0.057(53)	

ΔG_v[a]	Type	$V_1V_2\ l_2V_3$[b]	$(P,\ l_2,\ i)$	G_v	B_v	$D_v \times 10^7$	$H_v \times 10^{12}$	Observed lines	n/N[c]	$Rms \times 10^3$
458										
6426.68295(44)	Σ–Σ	0003e– 0000e	(12 0 1)	6426.68295(44)	0.3861215(14)	1.566(10)	0.16(10)	P62/R59	100/109	0.9
6387.10682(59)	Π–Π	0113e – 0110e	(13 1 1)	6957.88482(59)	0.3863883(15)	1.6061(70)		P47/R49	55/65	1.1
6387.10575(62)		0113f – 0110f		6957.88375(62)	0.3870902(29)	1.693(32)	2.64(96)	P45/R49	60/67	1.6
457										
6436.28877(49)	Σ–Σ	0003e –0000e	(12 0 1)	6436.28877(49)	0.3969502(17)	1.669(10)		P42/R41	62/67	0.8
6396.2868(11)	Π–Π	0113e – 0110e	(13 1 1)		0.3971916(64)	1.693(80)		P28/R27	24/25	1.6
6396.2747(13)		0113f – 0110f			0.3987103(64)	2.964(63)		P21/R30	19/20	1.2
548										
6492.21192(53)	Σ–Σ	0003e – 0000e	(12 0 1)	6492.21192(53)	0.372525(26)	1.558(30)	1.49(89)	P50/R41	71/73	1.3
547										
6325.40822(71)	Σ–Σ	0003e – 0000e	(12 0 1)	6325.40822(71)	0.3846207(38)	0.499(38)		P32/R30	44/45	1.2

* The spectroscopic parameters were re-determined by fitting the combination differences.

[a] Difference between the upper and lower vibrational term values.

[b] Normal mode labeling according to the maximum value of the modulo of the expansion coefficients of an eigenfunction.

[c] *n*: number of transitions included in the fit; *N*: number of assigned rotational transitions.

Table 7

Summary of the global line position fits for N_2O-456 and 546 isotopologues.

Isotopologue	N_{data}[a]	Range (cm^{-1})	N_{par}[b]	χ_{fit}	RMS (cm^{-1})
456	30,298	12 – 12,640	133	1.18	0.0013
546	33,305	13 – 12,774	151	1.67	0.0018

[a] Number of the observed line positions involved to the fit.

[b] Number of the adjusted effective Hamiltonian parameters.

4.2. The 546 isotopologue

The input datafile includes observed line positions collected from the literature [1–4,6–13,15–20,25,27–29] and those obtained in this work. The file contains near 33,300 lines and covers 13 – 12,774 cm^{-1} spectral range. A summary of the datafile is given in Table 9. As the initial set of the effective Hamiltonian parameters we used the set published in our previous paper [21]. With 151 parameters we have reached the global RMS=0.0018 cm^{-1}. The weighted standard deviation of the fit is χ =1.67. This is slightly

Table 8

Source-by-source analysis of the experimental data and statistics of the line position fit for N_2O-456.

Data source	Type of spectrum[a]	Accuracy[b] ($10^{-3}\ cm^{-1}$)	N_{fit}	Spectral range (cm^{-1})		RMS_{fit} ($10^{-3}\ cm^{-1}$)
Andreev et al [15]	MW	0.0017	22	12.6	18.5	0.0024
Drouin and Maiwald [7]	MW	0.003	8	28.5	54.3	0.0091
Morino et al [6]	MW	0.00066	2	20.9	22.6	0.0015
Toth [4]	CALC	1.0	2430	529.8	5085.7	1.19
Toth [17,19]	FTS	0.06	254	1102.7	2216.5	0.08
Wang et al [3]	FTS	1.0	11583	1214.1	3465.3	1.05
Hinz et al [18]	HET	2.0-8.0	4	1257.4	1316.1	1.855
Guelachvili and Rao [16]	FTS	0.13	115	2112.0	2739.3	0.06
Toth [20]	FTS	0.06	271	2386.8	3463.5	0.15
Krell and Sams [5]	FTS	3.0	80	2391.6	2578.2	1.64
Ni et al [1]	FTS	1.0	10953	3496.1	8857.1	1.21
Amiot [13]	FTS	2.0	995	3582.7	5553.1	0.83
Herbin et al [8]	ICLAS	1.0	138	3910.7	4021.6	0.98
Liu et al [10,11]	CRDS	2.0	748	5906.4	6791.7	1.83
Wang et al [9]	FTS	2.0	45	6402.6	6462.9	2.20
Lu et al [28]	CRDS	1.0	565	6990.3	7665.1	1.45
Liu et al [12]	CRDS	1.0	23	7029.7	7065.2	1.05
Liu et al [27]	CRDS	1.0	81	7648.1	7896.9	1.40
Karlovets et al [29]	CRDS	1.0	215	7916.0	8375.3	2.47
Song et al [25]	CRDS	1.0	71	12559.5	12640.9	0.92
This work	CRDS	2.0	1695	6277.3	6498.5	2.81

[a] MW – microwave measurements, HET – laser heterodyne measurements, FTS – Fourier transform measurements, ICLAS – intra-cavity laser absorption measurements, CRDS – cavity ring down measurements, CALC – calculated line positions.

[b] Number of the fitted lines from the respective source.

Table 9

Source-by-source analysis of the experimental data and statistics of the line position fit for N_2O-546.

Data source	Type of spectrum[a]	Accuracy (10^{-3} cm^{-1})	N_{fit}[b]	Spectral range (cm^{-1})		RMS$_{fit}$ (10^{-3} cm^{-1})
Andreev et al [15]	MW	0.0017	22	13.0	18.7	0.0054
Morino et al [6]	MW	0.00066	2	21.0	22.7	0.0013
Drouin and Maiwald [7]	MW	0.003	7	29.9	54.1	0.0097
Toth [4]	CALC	1.0	2109	540.6	4703.0	1.02
Guelachvili and Rao [16]	FTS	0.5	569	585.3	2772.4	0.70
Toth [17,19]	FTS	0.06	264	1115.3	2240.4	0.12
Wang et al [3]	FTS	1.0	12168	1214.3	3626.6	1.37
Hinz et al [18]	HET	0.1	3	1257.4	1295.5	0.05
Ni [1]	FTS	1.0	610	1842.0	8640.4	1.80
Toth [20]	FTS	0.04	88	2143.6	3465.7	0.11
Toth [4]	FTS	0.06	324	2391.4	3474.4	0.59
Song et al [2]	FTS	1.0	13323	3475.0	8894.5	2.00
Amiot [13]	FTS	2.0	646	3582.6	5080.9	1.39
Herbin et al [8]	ICLAS	1.0	130	3953.1	4033.3	1.14
Liu et al [10,11]	CRDS	2.0	734	5906.0	6812.1	2.66
Liu et al [12]	CRDS	2.0	95	6913.3	7064.7	2.03
Lu et al [28]	CRDS	1.0	643	6913.3	7715.9	1.92
Liu et al [27]	CRDS	1.0	143	7648.3	7914.4	1.15
Karlovets et al [29]	CRDS	1.0	258	7916.1	8308.5	2.79
Song et al [25]	CRDS	1.0	72	12688.0	12774.0	2.21
This work	CRDS	2.0	1190	6291.3	6511.6	2.90

[a] MW – microwave measurements, HET – laser heterodyne measurements, FTS – Fourier transform measurements, ICLAS – intracavity laser absorption measurements, CRDS – cavity ring down measurements, CALC – calculated line positions.

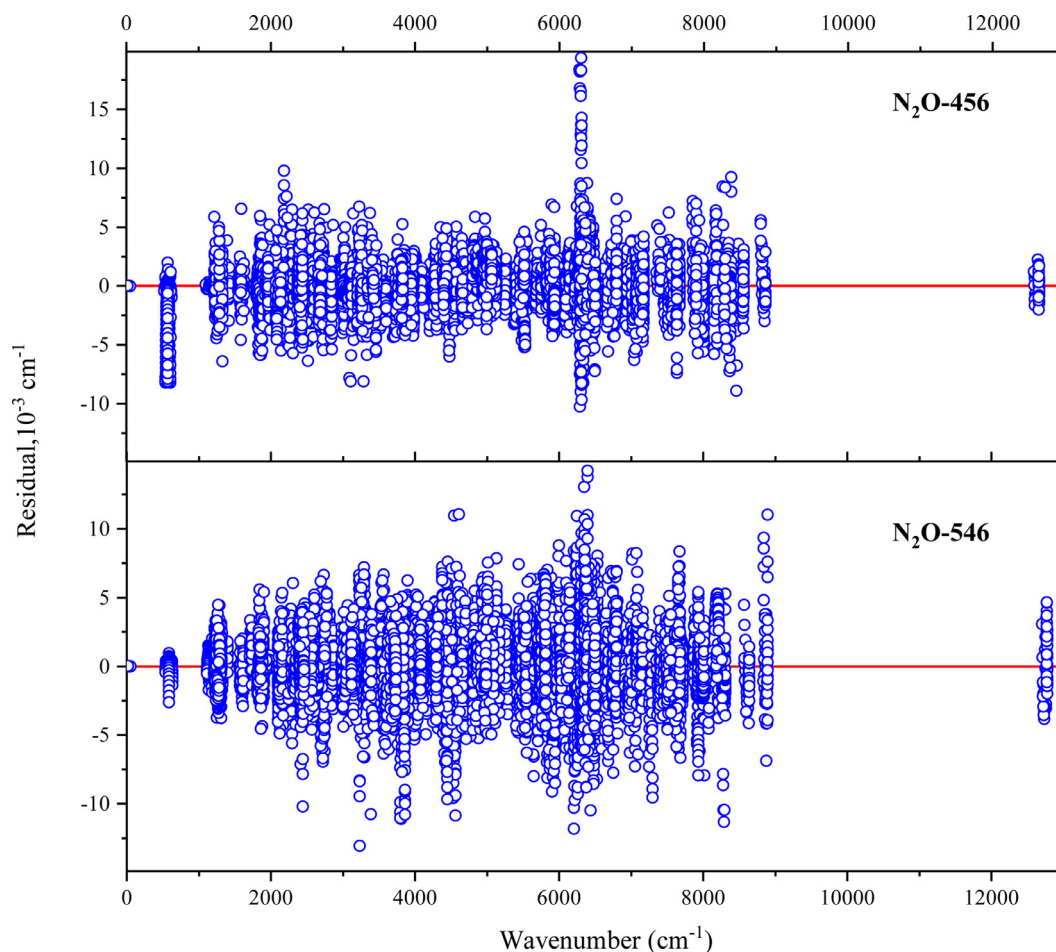[b] Number of the fitted lines from the respective source.

Fig. 3. Residuals of the line position fit for the N_2O-456 (upper panel) and N_2O-546 (lower panel) isotopologues.

worse than it was reached for the 456 isotopologue. It is because more bands are perturbed by interpolyad resonance interactions in the case of this isotopologue compared to 456. 2428 badly measured or strongly perturbed lines were excluded from the fit. In the lower panel of Fig. 3 the residuals are plotted versus wavenumber. The fitted set of the effective Hamiltonian parameters is presented as Supplementary Material.

5. Conclusion

In the present paper, we have studied the high resolution spectra of ^{15}N enriched N_2O in the 6277 – 6512 cm^{-1} range using CW-CRDS spectrometer. Eight and ten vibrational states respectively for the N_2O-456 and 546 isotopologues were studied for the first time. The effective Hamiltonian parameters for these isotopologues were improved by inclusion into the fit newly observed data and those which were not used in the previous fits. Six bands of the minor isotopologues 458, 548, 457 and 547 were observed in the studied wavenumber region for the first time.

Acknowledgement

Supplementary materials

Supplementary material associated with this article can be found, in the online version, at doi:10.1016/j.jqsrt.2019.04.035.

References

[1] Ni H-Y, Tashkun SA, Wang L, Perevalov VI, Song K-F, Liu A-W, et al. Fourier-transform spectroscopy of $^{14}N^{15}N^{16}O$ in the 3800 – 9000cm$^-$ region and global modeling of its absorption spectrum. J Mol Spectrosc 2007;248:41–60. doi:10.1016/j.jms.2007.11.011.

[2] Song KF, Liu AW, Ni HY, Hu SM. Fourier-transform spectroscopy of $^{15}N^{14}N^{16}O$ in the 3500-9000 cm^{-1} region. J Mol Spectrosc 2009;255:24–31. doi:10.1016/j.jms.2009.02.008.

[3] Wang CY, Liu AW, Perevalov VI, Tashkun SA, Song KF, Hu SM. High-resolution infrared spectroscopy of $^{14}N^{15}N^{16}O$ and $^{15}N^{14}N^{16}O$ in the 1200-3500 cm^{-1} region. J Mol Spectrosc 2009;257:94–104. doi:10.1016/j.jms.2009.06.012.

[4] Toth RA. Linelist of N_2O parameters from 500 to 7500 cm^{-1}. http://mark4sun.jpl.nasa.gov/n2o.html.

[5] Krell JM, Sams RL. Vibration-rotation bands of nitrous oxide: 4.1 μm region. J Mol Spectrosc 1974;51:492–507. doi:10.1016/0022-2852(74)90203-3.

[6] Morino I, Fabian M, Takeo H, Yamada KMT. High- J Rotational Transitions of NNO measured with the NAIR terahertz spectrometer. J Mol Spectrosc 1997;185:142–6. doi:10.1006/jmsp.1997.7366.

[7] Drouin BJ, Maiwald FW. Extended THz measurements of nitrous oxide, N_2O. J Mol Spectrosc 2006;236:260–2. doi:10.1016/j.jms.2006.01.005.

[8] Herbin H, Picqué N, Guelachvili G, Sorokin E, Sorokina IT. N^2O weak lines observed between 3900 and 4050 cm^{-1} from long path absorption spectra. J Mol Spectrosc 2006;238:256–9. doi:10.1016/j.jms.2006.05.004.

[9] Wang L, Perevalov VI, Tashkun SA, Gao B, Hao LY, Hu SM. Fourier transform spectroscopy of N_2O weak overtone transitions in the 1-2 μm region. J Mol Spectrosc 2006;237:129–36. doi:10.1016/j.jms.2006.03.007.

[10] Liu AW, Kassi S, Malara P, Romanini D, Perevalov VI, Tashkun SA, et al. High sensitivity CW-cavity ring down spectroscopy of N_2O near 1.5 μm (I). J Mol Spectrosc 2007;244:33–47. doi:10.1016/j.jms.2007.01.007.

[11] Liu AW, Kassi S, Perevalov VI, Tashkun SA, Campargue A. High sensitivity CW-Cavity ring down spectroscopy of N_2O near 1.5 μm (II). J Mol Spectrosc 2007;244:48–62. doi:10.1016/j.jms.2007.05.010.

[12] Liu AW, Kassi S, Perevalov VI, Hu SM, Campargue A. High sensitivity CW-cavity ring down spectroscopy of N_2O near 1.5 μm (III). J Mol Spectrosc 2009;254:20–7. doi:10.1016/j.jms.2008.12.006.

[13] Amiot C. Vibration-rotation bands of $^{14}N^{15}N^{16}O$ and $^{15}N^{14}N^{16}O$: 1.6–5.7 μm region. J Mol Spectrosc 1976;59:191–208. doi:10.1016/0022-2852(76)90290-3.

[14] Amiot C. Vibration-rotation bands of $^{15}N_2^{16}O$ and $^{14}N_2^{18}O$. J Mol Spectrosc 1976;59:380–95. doi:10.1016/0022-2852(76)90019-9.

[15] Andreev BA, Burenin AV, Karyakin EN, Krupnov AF, Shapin SM. Submillimeter wave spectrum and molecular constants of N_2O. J Mol Spectrosc 1976;62:125–48. doi:10.1016/0022-2852(76)90344-1.

[16] Guelachvili G, Narahari Rao K. Handbook of infrared standards, with spectral maps and transition assignments between 3 and 260 um. Florida: Academic Press Orlando; 1986. p. 32887.

[17] Toth RA. Frequencies of N_2O in the 1100 to 1440 cm$^-$ region. J Opt Soc Am B 1986;3:1263. doi:10.1364/JOSAB.3.001263.

[18] Hinz A, Wells JS, Maki AG. Heterodyne measurements of hot bands and isotopic transitions of N_2O Near 7 . 8 lam. Z Phys D 1987;5:351–8.

[19] Toth RA. N_2O vibration–rotation parameters derived from measurements in the 900–1090 and 1580 – 2380 cm$^-$ regions. J Opt Soc Am B 1987;4:357. doi:10.1364/JOSAB.4.000357.

[20] Toth RA. Line-frequency measurements and analysis of N_2O between 900 and 4700 cm$^-$. Appl Opt 1991;30 5289. doi:10.1364/AO.30.005289.

[21] Tashkun SA, Perevalov VI, Kochanov R V, Liu AW, Hu SM. Global fittings of $^{14}N^{15}N^{16}O$ and $^{15}N^{14}N^{16}O$ vibrational-rotational line positions using the effective Hamiltonian approach. J Quant Spectrosc Radiat Transf 2010;111:1089–105. doi:10.1016/j.jqsrt.2010.01.010.

[22] Kang P, Wang J, Liu GL, Sun YR, Zhou ZY, Liu AW, et al. Line intensities of the 30011e – 00001e band of $^{12}C^{16}O_2$ by laser-locked cavity ring-down spectroscopy. J Quant Spectrosc Radiat Transf 2018;207:1–7. doi:10.1016/j.jqsrt.2017.12.013.

[23] Wang J, Sun YR, Tao LG, Liu AW, Hu SM. Communication: molecular near-infrared transitions determined with sub-kHz accuracy. J Chem Phys 2017:147. doi:10.1063/1.4998763.

[24] Gao B, Jiang W, Liu AW, Lu Y, Cheng CF, Cheng GS, et al. Ultrasensitive near-infrared cavity ring-down spectrometer for precise line profile measurement. Rev Sci Instrum 2010;81:1–5. doi:10.1063/1.3385675.

[25] Song K-F, Gao B, Liu A-W, Perevalov VI, Tashkun SA, Hu S-M. Cavity ring-down spectroscopy of the bands of ^{15}N substituted N_2O. J Quant Spectrosc Radiat Transf 2010;111:2370–81. doi:10.1016/j.jqsrt.2010.05.022.

[26] Teffo JL, Perevalov VI, Lyulin OM. Reduced effective Hamiltonian for a global treatment of Rovibrational energy levels of Nitrous Oxide. J Mol Spectrosc 1994;168:390–403. doi:10.1006/jmsp.1994.1288.

[27] Liu AW, Kassi S, Perevalov VI, Tashkun SA, Campargue A. High sensitivity CW-Cavity ring down spectroscopy of N_2O near 1.28 μm. J Mol Spectrosc 2011;267:191–9. doi:10.1016/j.jms.2011.03.025.

[28] Lu Y, Mondelain D, Liu AW, Perevalov VI, Kassi S, Campargue A. High sensitivity CW-Cavity ring down spectroscopy of N_2O between 6950 and 7653cm$^-$ (1.44–1.31 μm): I. Line positions. J Quant Spectrosc Radiat Transf 2012;113:749–62. doi:10.1016/j.jqsrt.2012.03.005.

[29] Karlovets E V, Campargue A, Kassi S, Perevalov VI, Tashkun SA. High sensitivity cavity ring down spectroscopy of N_2O near 1.22 μm: (I) rovibrational assignments and band-by-band analysis. J Quant Spectrosc Radiat Transf 2016;169:36–48. doi:10.1016/j.jqsrt.2015.09.012.

[30] Tashkun SA, Tyuterev VG. In: Nadezhdinskii AI, Ponomarev YV, Sinitsa LN, editors. GIP: a program for experimental data reduction in molecular spectroscopy, 2205. 11th Symp. Sch. High-Resolution Mol. Spectrosc.; 1994. p. 188. doi:10.1117/12.166203.